

## THE CLEO-c PHYSICS PROGRAM

Thomas E. Coan

*Physics Department, Southern Methodist University, Dallas, TX 75275, USA*

*E-mail: coan@mail.physics.smu.edu*

### Abstract

The CLEO collaboration at the Cornell Electron Storage Ring (CESR) is proposing a three-year experiment that specifically emphasizes charm and QCD studies in the energy range  $\sqrt{s} = 3\text{--}5$  GeV, utilizes the existing detector and requires minimal modification of CESR to produce a luminosity  $\mathcal{L} = (1\text{--}5) \times 10^{32} \text{ cm}^{-2}\text{sec}^{-1}$ . Key features of this “CLEO-c” physics program are summarized.

## 1 Introduction

The impressive performance of the asymmetric B-factories at KEK and SLAC in the  $\Upsilon(4S)$  region and the large integrated luminosities ( $\sim 400 \text{ fb}^{-1}$ ) the corresponding detectors, Belle and BaBar, are projected to collect in the next few years renders additional contributions to B-meson physics by CLEO problematic. Correspondingly, CLEO seeks to exploit its extensive experience in heavy flavor physics and the excellent performance of its nearly hermetic detector to perform focused studies of charm and QCD physics in the energy range  $\sqrt{s} = 3 - 5 \text{ GeV}$ . Indeed, CLEO no longer runs at  $\sqrt{s} \sim \Upsilon(4S)$  but began a year long program in November 2001 to run at  $\sqrt{s} = \Upsilon(1S), \Upsilon(2S), \Upsilon(3S)$  and to collect  $\int \mathcal{L} dt = 1 - 2 \text{ fb}^{-1}$  at each resonance. This data set is a factor of 10 – 20 larger than the existing world data set of similar type and will provide 2 – 3% measurements of leptonic widths and precise measurements of a wide range of precision branching fractions to complement the proposed QCD studies <sup>1)</sup>.

The CLEO-c proposal <sup>2)</sup> entails a 3-year run plan at “charm production” threshold: running at  $\sqrt{s} = \Psi(3770)$  ( $D\bar{D}$  threshold) in 2003 and collecting  $\int \mathcal{L} dt = 3 \text{ fb}^{-1}$ ; running in 2004 at  $\sqrt{s} \sim 4100 \text{ MeV}$  ( $D_s\bar{D}_s$  threshold) and collecting  $\int \mathcal{L} dt = 3 \text{ fb}^{-1}$ ; and running in 2005 at  $\sqrt{s} = J/\Psi(3100)$  and collecting  $\int \mathcal{L} dt = 1 \text{ fb}^{-1}$ . These integrated luminosities represent data sets that are a factor of 15 – 500 larger than corresponding data sets of BES II and MARK III.

A focussed set of precision measurements of charm absolute branching fractions and spectroscopy of  $c\bar{c}$  quarkonia is the core of the CLEO-c physics program. The physics reach has been carefully simulated using analysis tools and detector understanding acquired by the CLEO collaboration from many years of heavy quark studies. Measurement of  $D$  and  $D_s$  leptonic decays permit determinations of the decays constants  $f_D$  and  $f_{D_s}$ , respectively. Measurements of semileptonic decays will yield precision determinations of semileptonic form factors and the CKM matrix elements  $V_{cd}$  and  $V_{cs}$  and so provide a check of the unitarity of the matrix itself. Semileptonic form factors can also be accurately determined. Precise charm absolute branching fractions will normalize important  $B$  decay measurements and provide a robust means of verifying and calibrating theoretical techniques of heavy quark effective theory (HQET) and lattice gauge theory that can in turn be applied to the  $b$  sector to improve measurements of CKM matrix elements  $V_{ub}, V_{cb}, V_{td}$  and  $V_{ts}$ .

High statistics samples of  $c\bar{c}$  data (as well as  $b\bar{b}$  data from the  $\Psi(nS)$  runs now underway) will permit efficient searches for purely gluonic “glueballs” and

quark-gluon “hybrids” in the mass range  $1.5 - 2.5 \text{ GeV}/c^2$ . The existence of such exotic states is an unambiguous prediction of QCD and the unambiguous detection of such states is of fundamental importance. Determination of the  $J^{PC}$  quantum numbers through partial wave analysis, as well as measurements of decay widths and branching fractions of putative exotic states, will clarify the gluonic content of exotic candidates. Additionally, CLEO-c will have sensitivity to physics beyond the Standard Model by mounting searches for  $D\bar{D}$ -mixing,  $CP$  violation in the charm sector, and searches for a host of rare  $D$  and  $\tau$  decays.

Minimal modifications to CESR are required to implement the lower energy running in the range  $\sqrt{s} = 3 - 5 \text{ GeV}$ . Supplemental radiation damping will be induced to produce transverse cooling by the insertion of 18 meters of 2 T wiggler magnets so that the luminosity scales as  $\mathcal{L} \sim s$  rather than the naive  $\mathcal{L} \sim s^2$  expectation. The design luminosity is  $\mathcal{L} = (1 - 5) \times 10^{32} \text{ cm}^{-2}\text{s}^{-1}$ , depending on  $\sqrt{s}$ , with an anticipated beam energy uncertainty  $\sigma_B \sim 1.2 \text{ MeV}$  at  $\sqrt{s} = J/\Psi$ . Prototype wiggler design and construction are well advanced.

## 2 Charm Threshold Running

CLEO-c will not be able to compete against the asymmetric  $B$  factory detectors running at  $\sqrt{s} = \Upsilon(4S)$  in the raw number of charm events collected. However, running at charm threshold production has distinct advantages over continuum  $e^+e^- \rightarrow c\bar{c}$  production. For example, the charged and neutral multiplicities in  $\Psi(3770)$  events are only 5.0 and 2.4, respectively, reducing combinatorics and leading to high detection efficiencies and low systematic errors. Additionally, charm events at threshold are pure  $D\bar{D}$ , including the  $\Psi(4140)$  decaying into  $D\bar{D}^*$ ,  $D_s\bar{D}_s$  and  $D_s\bar{D}_s^*$ . No additional particles from fragmentation are produced.

Low multiplicity events and pure  $D\bar{D}$  states, coupled with the relatively high branching fractions typical of  $D$  decays, permit the efficient implementation of “double tag” studies where one  $D$  is fully reconstructed and the other is studied in a bias free fashion. This permits the determination of absolute branching fractions with very low backgrounds. In leptonic and semileptonic decays, the missing neutrino can be treated as a missing mass problem, with a missing mass resolution better than one pion mass. Finally, the quantum coherence of the  $D\bar{D}$  states produced in  $\Psi(3770) \rightarrow D\bar{D}$  and  $\Psi(4140) \rightarrow \gamma D\bar{D}$  decays permit relatively simple techniques<sup>3)</sup> for measuring  $D\bar{D}$  mixing parameters and direct  $CP$  violation.

### 3 Absolute Branching Fractions

The combination of pure  $D\bar{D}(D_s\bar{D}_s)$  at  $\sqrt{s} = \Psi(3770)$  ( $\sqrt{s} = 4140$  MeV), typical charm branching fractions of (1 – 15)%, and a high reconstruction efficiency for  $D$ -mesons, lead to a high net  $D$ -meson tagging efficiency of  $\sim 15\%$  for CLEO-c. Key selection criteria for  $D$  candidates include constraints on the energy difference between the  $D$  candidate and the beam energy, the beam constrained mass of the  $D$  candidate, and particle identification cuts. Figure 1 shows the reconstructed  $D^0$  mass for simulated  $D^0 \rightarrow K^-\pi^+$  decays (left) and the reconstructed  $D_s$  mass for the  $D_s \rightarrow K^+K^-\pi^+$  mode. Only  $1 \text{ fb}^{-1}$  out of the target  $3 \text{ fb}^{-1}$  of integrated luminosity is plotted and the effects of sequential selection cuts are indicated. Note the logarithmic vertical scale.

The technique for tagging a single  $D$  candidate can of course be extended to the second  $D$ -meson candidate in  $e^+e^- \rightarrow c\bar{c}$  threshold production events by essentially applying the single-tag technique twice. Some additional constraints on the flavor-defining charge of the second  $D$  candidate, overall event topology, and overall event energy and invariant mass are applied to produce “double-tag”  $D$  candidates. Using a modified version of a technique developed at MARK III <sup>4)</sup>, CLEO-c can then precisely measure absolute hadronic charm meson branching fractions using double-tag events. Figure 2 shows the reconstructed  $D$  mass from the  $D^0 \rightarrow K^-\pi^+$  mode (left) and from the  $D^+ \rightarrow K^-\pi^+\pi^+$  mode. In both cases the distribution is made after another  $D$  of the opposite flavor has been found in the event and only  $1 \text{ fb}^{-1}$  of simulated data out of the anticipated  $3 \text{ fb}^{-1}$  is used. Note the almost complete absence of background in both distributions. Table 1 compares the branching fraction precision for some key  $D$  decay modes anticipated with  $3 \text{ fb}^{-1}$  of CLEO-c data and the corresponding PDG 2000 values.

Table 1: *Branching fraction precision of key  $D$  decay modes projected for  $3 \text{ fb}^{-1}$  of CLEO-c data compared to PDG 2000 values.*

Mode	$\sqrt{s}$ (GeV)	$(\frac{\delta Br}{Br})_{PDG}$	$(\frac{\delta Br}{Br})_{CLEO-c}$
$D^0 \rightarrow K^-\pi^+$	3770	2.4%	0.6%
$D^+ \rightarrow K^-\pi^+\pi^+$	3770	7.2%	0.7%
$D_s \rightarrow \phi\pi$	4140	25%	1.9%

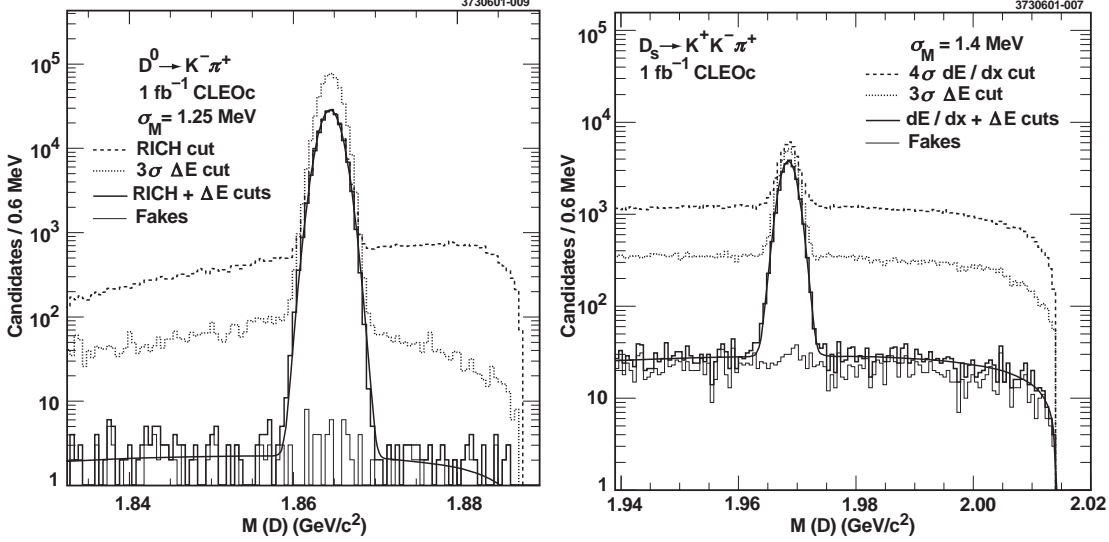


Figure 1: Reconstructed  $D$  mass in simulated  $D^0 \rightarrow K^- \pi^+$  decays (left) and  $D_s \rightarrow K^+ K^- \pi^+$  decays (right) with CLEO-c.

#### 4 Leptonic and Semileptonic Decays

Precision measurements of leptonic and semileptonic decays in the charm sector are vital for determining CKM matrix elements that describe the mixing of flavors and generations induced by the weak interaction. The lowest order expression for the leptonic branching fraction of a  $D$ -meson is given by <sup>5)</sup>

$$\mathcal{B}(D_q \rightarrow l\nu) = \frac{G_F^2}{8\pi} m_{D_q} m_l^2 \left(1 - \frac{m_l^2}{m_{D_q}^2}\right) f_{D_q}^2 |V_{cq}|^2 \tau_{D_q}, \quad (1)$$

where  $f_{D_q}$  is the parameter that encapsulates the strong physics of the process and  $|V_{cq}|$  is the CKM matrix parameter that encapsulates the weak physics and quantifies the amplitude for quark mixing. Measurements of leptonic branching fractions can then be used to extract  $f_{D_q}$  and, with additional semileptonic measurements,  $|V_{cq}|$ . They will exploit fully tagged  $D^+$  and  $D_s$  decays from running at the  $\Psi(3770)$  and  $\sqrt{s} \sim 4140$  MeV.  $D_q \rightarrow \mu\nu$  decays are detected in tagged events by observing a single track of the correct charge, missing energy, and accounting for any residual energy in the calorimeter.

Figure 3 shows the reconstructed missing mass squared for  $D^+ \rightarrow \mu\nu$  (left) and  $D_s \rightarrow \mu\nu$  decays. Note the signal (shaded area) is cleanly separated from

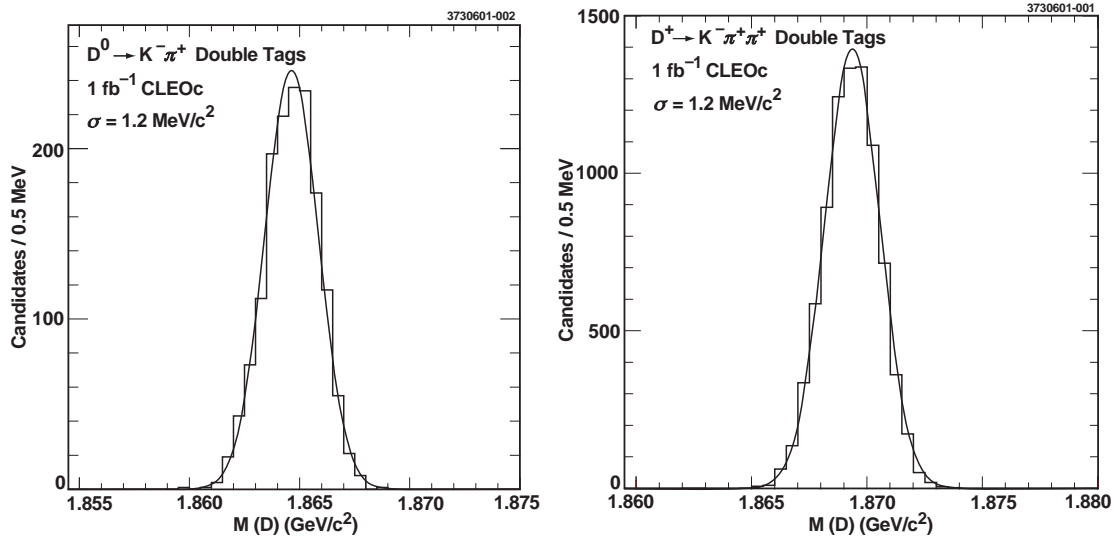


Figure 2: Reconstructed  $D$  mass in the  $D^0 \rightarrow K^- \pi^+$  decay mode (left) and in  $D^+ \rightarrow K^- \pi^+ \pi^+$  (right). A  $D$  candidate of the opposite flavor has also been found in each event.

the background. The decay  $D_s \rightarrow \tau \nu$  is more complicated to treat because of the secondary decay of the  $\tau$  but still fully accessible to CLEO-c. Table 2 compares with PDG 2000 values the expected precision for  $D$ -meson decay constants with  $3 \text{ fb}^{-1}$  of data and assuming 3 generation unitarity.

Table 2: Charm decay constant precision expected with  $3 \text{ fb}^{-1}$  of CLEO-c data compared to PDG 2000 values.

Decay Constant	Mode (GeV)	$(\frac{\delta f}{f})_{PDG}$	$(\frac{\delta f}{f})_{CLEO-c}$
$f_{D_s}$	$D_s^+ \rightarrow \mu \nu$	17%	1.9%
$f_{D_s}$	$D_s^+ \rightarrow \tau \nu$	33%	1.7%
$f_D$	$D^+ \rightarrow \mu \nu$	Upper limit	2.3%

The differential semileptonic decay rate for a  $D$ -meson to a pseudoscalar  $P$  is given by <sup>6)</sup>

$$\frac{d\Gamma(D \rightarrow P l \nu)}{dq^2} = \frac{G_F^2}{24\pi^3} |V_{cq}|^2 p_P^3 |f(q^2)|^2, \quad (2)$$

where the form factor  $f(q^2)$  encapsulates the strong physics. Form factor measure-

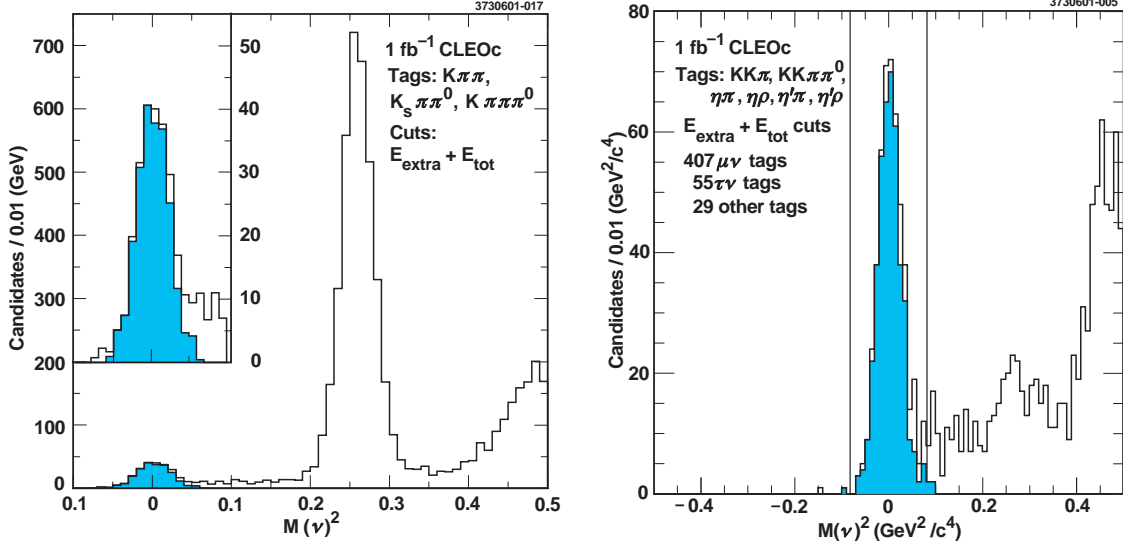


Figure 3: Reconstructed missing mass squared for simulated  $D^+ \rightarrow \mu\nu$  candidates (left) and for  $D_s \rightarrow \mu\nu$  candidates (right). The shaded areas are the signal.

ments are a key means to test theory's description of heavy quark decays. Precision measurements in inclusive semileptonic decays can strenuously test heavy quark effective theory (HQET) <sup>7)</sup> while exclusive decays are a rigorous testbed for Lattice QCD (LQCD) calculations <sup>8)</sup>. More progress in heavy quark decay theory is necessary to extract precision values ( $\delta V/V \sim 5\%$ ) of the CKM matrix elements  $|V_{td}|$  and  $|V_{ts}|$  from data at present and planned  $B$  physics experiments.

Figure 4 shows on the left the reconstruction of the mode  $D^0 \rightarrow \pi^- e^+ \nu$  where the horizontal axis is the difference  $U$  between missing energy  $E_{\text{miss}}$  and missing momentum  $P_{\text{miss}}$ . The signal (shaded area) is well separated from the far more abundantly produced  $D^0 \rightarrow K^- e^+ \nu$  decays. The right hand side shows a measurement of the form factor in the same  $D^0 \rightarrow \pi^- e^+ \nu$  decay and the line is a fit to the simulated data using the parameterization  $f = f(0)e^{\alpha q^2}$ . Table 3 shows the expected precision in branching fraction  $\mathcal{B}$  for some important semileptonic decays with CLEO-c for an integrated luminosity of  $3 \text{ fb}^{-1}$  and the comparison with PDG 2000 values.

The absolute branching fraction for a semileptonic  $D$  decay to a pseudoscalar can be combined with a measurement of the  $D$  lifetime  $\tau_D$  to yield the

Table 3: *Expected precision in the branching fraction  $\mathcal{B}$  for important semileptonic decays with CLEO-c and the comparison with PDG 2000 values.*

Mode	$(\frac{\delta\mathcal{B}}{\mathcal{B}})_{PDG}$	$(\frac{\delta\mathcal{B}}{\mathcal{B}})_{CLEO-c}$
$D^0 \rightarrow K^- e^+ \nu$	5%	0.4%
$D^0 \rightarrow \pi^- e^+ \nu$	16%	1.0%
$D^+ \rightarrow \pi^0 e^+ \nu$	48%	2.0%
$D_s \rightarrow \phi e^+ \nu$	25%	3.1%

total decay width:

$$\Gamma(D \rightarrow Pl\nu) = \frac{\mathcal{B}(D^0 \rightarrow Pl\nu)}{\tau_D} = \beta_{cq} V_{cq}, \quad (3)$$

with  $\beta_{cq}$  given by theory. Using eqs. 1, 2 and 3 and combining measurements from leptonic and semileptonic decays make it possible to measure charm decays constants directly, without the assumption of 3-generation unitarity, and to then determine the CKM matrix elements  $|V_{cd}|$  and  $|V_{cs}|$ , also without the unitarity assumption. Table 4 shows the expected precision in  $V_{cd}$  and  $V_{cs}$  for CLEO-c with  $3 \text{ fb}^{-1}$  of integrated luminosity.

Table 4: *Expected precision in  $V_{cq}$  matrix elements with CLEO-c and the comparison to PDG 2000 values.*

$\frac{\delta V}{V}$	CLEO-c	PDG 2000
$\frac{\delta V_{cd}}{V_{cd}}$	1.6%	7%
$\frac{\delta V_{cs}}{V_{cs}}$	1.7%	11%

## 5 QCD Probes

CLEO-c will probe the low-energy nonperturbative structure of QCD with new precision. QCD predicts the existence of bound hadronic states in the mass range  $\sim (1.5 - 2.5) \text{ GeV}/c^2$  in which gluons are both constituents and the source of the binding force. Both fully gluonic “glueballs” and quark-gluon “hybrids” are novel forms of matter whose existence has yet to be unambiguously demonstrated. Their detection and study will be a major focus of  $J/\Psi$  running. With an expected CESR luminosity of  $\mathcal{L} = 2 \times 10^{32} \text{ cm}^2/\text{sec}^{-1}$  at  $\sqrt{s} = J/\Psi$ , CLEO-c expects to collect  $1 \times 10^9$   $J/\Psi$  events.



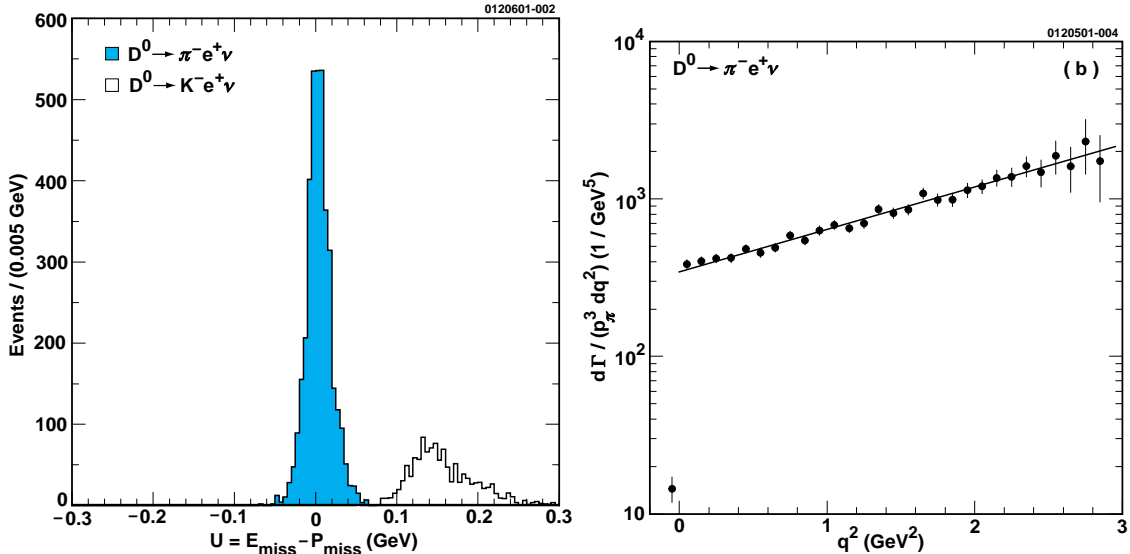


Figure 4: Reconstructed  $D^0 \rightarrow \pi^- e^+ \nu$  decays (left) as a function of the quantity  $U$  described in the text. The signal is the shaded area. A measurement of the form factor in the same decay mode with a line fit to the data points (right).

Radiative  $J/\Psi$  decays are a fruitful environment to search for glue rich hadronic matter <sup>9)</sup> and CLEO-c will collect roughly 60 million  $J/\Psi \rightarrow \gamma X$  decays with its projected  $1 \text{ fb}^{-1}$  of integrated luminosity from  $J/\Psi$  running. The excellent energy resolution ( $\sigma_E = 4 \text{ MeV}$  at  $E_\gamma = 100 \text{ MeV}$ ) and large solid angle coverage of CLEO's calorimeter will permit efficient use of partial wave analyses to determine absolute branching fraction for scalar resonances  $X \rightarrow \pi\pi, KK, \eta\eta, p\bar{p}$ .

For example, with CLEO-c's projected data set and if the branching fraction measurements from BES <sup>10)</sup> are indeed correct for the  $f_J(2220)$ , then CLEO-c will see many thousands of events in a variety of exclusive  $f_J(2220)$  decay modes. Figure 5 shows the invariant mass spectrum for  $J/\Psi \rightarrow \gamma\pi^+\pi^-$  (left) and for  $J/\Psi \rightarrow \gamma K^+K^-$ . Using only 1/6 of the projected data set, the  $f_J(2220)$  is clearly distinguishable from the hadronic and radiative backgrounds indicated by the shaded regions. Firmly establishing or debunking the existence of the  $f_J(2220)$  is a CLEO-c priority.

The inclusive photon spectrum from radiative  $J/\Psi$  decays is also a powerful means to search for new glue-rich hadronic states. As an example, Figure 6 shows such an inclusive photon spectrum for only 60 million  $J/\Psi$  decays under the

assumption  $\mathcal{B} \rightarrow \gamma f_J(2220) = 8 \times 10^{-4}$ . The  $f_J(2220)$  peak is clearly visible from the hadronic  $J/\Psi$  background shown as the shaded region. Due to its nearly hermetic structure (93% of  $4\pi$ ), the CLEO-c detector is highly efficient at rejecting events of the type  $J/\Psi \rightarrow \pi^0 X$  where one of the photons from the  $\pi^0$  gets lost. With its projected data set of  $10^9$   $J/\Psi$  events, CLEO-c should be able to detect any narrow resonances in radiative  $J/\Psi$  decays with a branching fraction of  $\mathcal{O}(10^{-4})$  or larger. An existing data set of  $25 \text{ fb}^{-1}$  of  $\gamma\gamma$  events will be a useful crosscheck for putative glue-rich states.

## 6 Detector Performance

The performance of the current CLEO detector is well-suited to the CLEO-c physics program. In some sense the detector is overdesigned since it was designed for running at  $\sqrt{s} = \Upsilon(4S)$ . Both the tracking system and the calorimeter cover 93% of  $4\pi$  steradians, providing the near hermeticity vital for partial wave analyses and for efficient background rejection. The central drift chamber has a fractional momentum resolution  $\sigma_p/p = 0.35\%$  at  $p = 1 \text{ GeV}/c$  and a  $D \rightarrow K\pi$  mass resolution  $\sigma \sim 6.3 \text{ MeV}$ . The CsI calorimeter has excellent energy resolution,  $\sigma_e/E = 2.2\%$  at  $E = 1 \text{ GeV}$  and  $5 - 7 \text{ MeV}$   $\pi^0$  mass resolution. The dedicated charged hadron identification system, a ring imaging Cherenkov detector that covers 83% of the full solid angle that is used in conjunction with  $dE/dx$  measurements from the drift chamber, provides  $10 - 200$  sigma  $K/\pi$  separation from  $470 \text{ MeV}$  up to the kinematic limit for  $D$  decay daughters at CLEO-c collision energies.

## 7 Summary

CLEO-c is a timely proposed experiment designed to make important measurements in charm physics and QCD with projected data sets many orders of magnitude larger than current world sets of comparable type. These measurements will provide important measurements of CKM matrix elements and strenuously test theory's description of heavy quark decay as well as QCD's prediction of exotic gluonic states of matter. Table 5 summarizes some important CLEO-c measurements, projecting  $3 \text{ fb}^{-1}$  of integrated luminosity, and compares them to the expected reach of the current asymmetric B-factories, assuming  $400 \text{ fb}^{-1}$  of integrated luminosity. The relative advantages of charm threshold running lead to favorable overall errors. The current CLEO detector is fully capable of providing measurements with the appropriate resolution in particle energy, tracking and charged hadron identification to accomplish CLEO-c physics goals.

Table 5: Comparison of the physics reach for some important measurements between CLEO-c and the asymmetric B-factories and PDG 2000 values.

	CLEO-c	B-factories	PDG
$f_D$	2.3%	10–20 %	–
$f_{D_s}$	1.7%	6–9%	19%
$\mathcal{B}(D^+ \rightarrow K\pi\pi)$	0.7%	3–5%	7%
$\mathcal{B}(D_s \rightarrow \phi\pi)$	1.9%	5–10%	25%
$\mathcal{B}(D_s \rightarrow K\pi)$	0.6%	2–3%	2%

## 8 Acknowledgements

I would like to thank the conference organizers for both the invitation and the conference's excellent organization. The assistance of I. Shipsey in the preparation of this talk is appreciated. The author's work is supported by the U.S. Dept. of Energy under contract DE-FG03-95ER40908.

## References

1. D. Besson and T. Skwarnicki, *Ann. Rev. nucl. Part. Sci.* **43** 333 (1993).
2. <http://www.lns.cornell.edu/public/CLEO/spoke/CLEOc/ProjDesc.html>
3. M. Gronau *et al*, hep-ph/0103110.
4. MARK III Collaboration, R.M. Baltrusaitis *et al*, *Phys. Rev. Lett.* **56**, 89 (1988).
5. J.L. Rosner, *Phys. Rev. D* **42**, 3732 (1990).
6. B.Grinstein *et al*, *Phys. Rev. Lett.* **56**, 298 (1986); F.J. Gilman and R.L. Singleton, *Phys Rev. D* **41**, 142 (1990); K. Hagiwara *et al*, *Nucl. Phys B* **327** 569 (1989).
7. I.I. Bigi *et al*, *Ann. Rev. Nucl. Part. Sci.* **47**, 591 (1997) and references therein.
8. Cornell Workshop on High-Precision Lattice QCD, January 2001.
9. T. Appelquist *et al*, *Phys. Rev. Lett.* **34**, 365 (1975); M.S. Chanowitz, *Phys. Rev. D* **12**, 918 (1975).
10. BES Collaboration, J.Z. Bai *et al*, *Phys. Rev. Lett.* **76**, 3502 (1996).

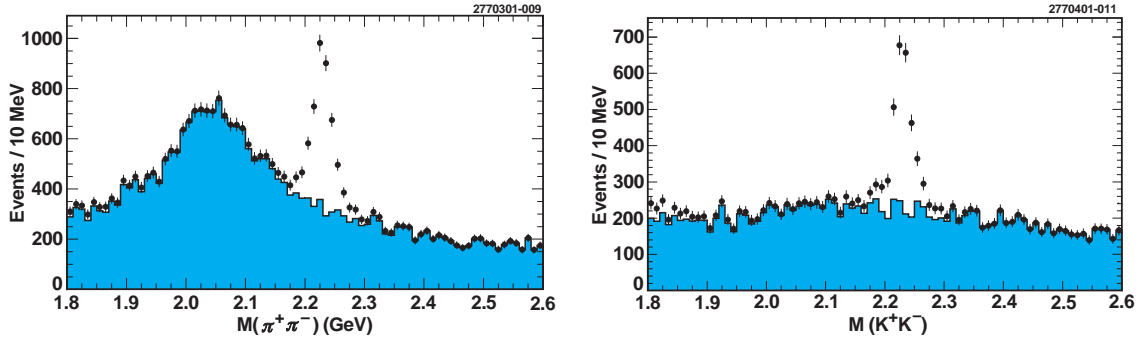


Figure 5: *Expected invariant mass spectrum with CLEO-c for  $J/\Psi \rightarrow \gamma\pi^+\pi^-$  (left) and  $J/\Psi \rightarrow \gamma K^+K^-$  (right). The shaded portion in each plot corresponds to hadronic and radiative backgrounds. The peaks are attributed to the  $f_J(2220)$ .*

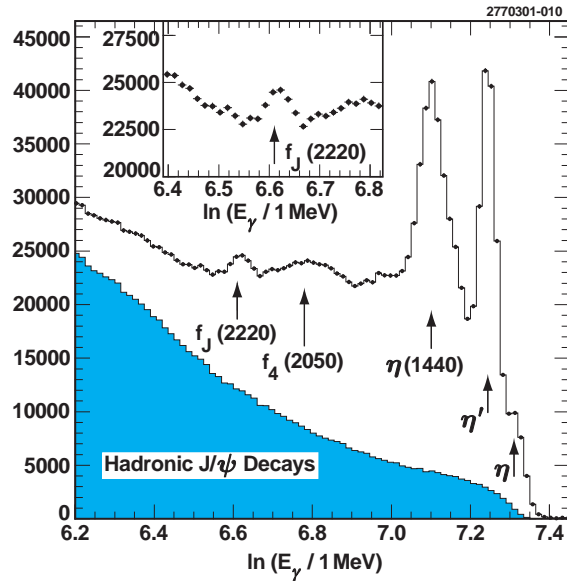


Figure 6: *The inclusive photon spectrum for radiative  $J/\Psi$  decays with CLEO-c. The shaded region shows the background from hadronic  $J/\Psi$  decays.*